Journal of Advanced Engineering Trends
ISSN : 2682 - 2091

Vol.44, No.1. January 2025

http://jaet.journals.ekb.eg

High gain 1x4 Slot Antenna array for 5G 28GHz Networks

Esraa Esam Elden [1,*], Ahmed A. Ibrahim[1], Abou- Hashema M. El-sayed [2], Ayat G. Aboelmagd [3]

[1] *Communications and Electronics Engineering Department, Faculty of Engineering, Minia University, Egypt.*

[2] *Communications and Electronics Engineering Department, Faculty of Engineering, Minia University, Egypt*

[3] *Elminya High institute for engineering and technology*

**Corresponding author(s).* Email: *ahmedabdel_monem@mu.edu.eg*

A R T I C L E I N F O

Article history:
Received:
Accepted:
Online:

Keywords:
Key 1: *slot antenna, High gain*
Key 2: *1x2 antenna array*
Key 3: *1x4 antenna array, 5G networks*

A B S T R A C T

This work introduces a high-gain slot antenna designed for the latest 5G networks, specifically operating at a frequency of 28 GHz. The antenna features a rectangular slot design, and its gain is significantly enhanced using 1x2 and 1x4 antenna arrays, resulting in an approximate increase of 4.2 dBi. The antenna has been fabricated and thoroughly tested, demonstrating operation within the frequency range of 26 GHz to 29.6 GHz with an S11 value of ≤ -10 dB, and achieving a gain of about 5 dBi across this band. The 1x2 and 1x4 antenna arrays have shown a bandwidth with S11 ≤ -10 dB ranging from 25.6 GHz to 29.8 GHz and 26.4 GHz to 29.9 GHz, respectively, attaining gains of 7.4 dBi at 28 GHz and 10.4 dBi at 28 GHz. The simulation and experimental results exhibit consistent patterns, confirming the proposed antenna's suitability for new 5G applications. All simulations were conducted using CST Microwave Studio.

1. Introduction

Every decade, new generations of mobile technology are introduced, driven by increasing data volumes, variety, and the rapid evolution of data consumption types. The next generation, 5G, is already being rolled out and will eventually replace the 4G networks that began in 2010. Transitioning to millimeter-wave (MMW) will be in a progressive way, leveraging the benefits of increased capacity, lower system latency, larger bandwidth, and a vast available spectrum [1-4]. The lower band and the higher band are considered the two primary frequency bands for 5G technology [5-7]. The mm-wave range, including 28 GHz and 38 GHz, is recognized as a potential standard for future 5G applications [8-12]. Utilizing more spectrum enables higher transmission speeds and capacity, though the corresponding frequencies are influenced by atmospheric attenuation, like rain and fog. These absorption difficulties may be handled by utilizing high-gain, highly directional antennas. [13-16]. Researchers have proposed several high-gain antenna designs, including antenna arrays with an artificial magnetic conductor (AMC) beneath the antenna [17-20], and the use of frequency selective surfaces (FSS) [21-25]. In the present research, 1x2, and 1x4 slot antenna arrays are created for gain enhancement. Using the 1x2 and 1x4 antenna arrays increases the antenna gain by approximately 4.2 dB. The fabricated antenna was tested, showing good agreement between simulated and experimental results. The 1x2 and 1x4 antenna arrays achieved bandwidths with S11 ≤ -10 dB, ranging from 25.4 GHz to 29.8 GHz and from 26.4 GHz to 30 GHz, respectively, and realized gains of about 7.4 dB at 27.3 GHz and 11.15 dB at 27.8 GHz. The proposed antenna demonstrates a compact size and suitable gain. The paper is arranged as: the first part provides an introduction and overview of 5G antenna improvement strategies. The second part describes the single antenna structure design. The third part describes the 1x2 antenna array. The fourth part describes the numerical results of the proposed 1x4 antenna array. The conclusion is offered in the fifth part.

Revised:11 September , 2024, Accepted:9 November , 2024

2. Single Antenna

Figure 1 depicts the 2D front and rear perspectives of the slot antenna arrangement. A 50 Ω microstrip line is mounted on a 4003 Rogers substrate, which has a dielectric constant of 3.35 and a thickness of 0.203 mm. The ground plane on the opposite side of the substrate is etched to create a rectangular slot. The design parameters include L=12 mm,a=3 mm, and b=2.6 mm, with the overall antenna dimensions being 12 mm x 12 mm. The end launcher connector is utilized in the simulation process as illustrated in Figure 1 to mimic the testing process. The design and simulation processes are conducted using CST Microwave Studio Software. The length of the microstrip line (denoted as d) is crucial for achieving optimal matching, as depicted in Figure 2. Any variation in microstrip length can influence the capacitance and inductance values of the transmission line, thereby affecting the antenna matching, as illustrated in Figure 2.

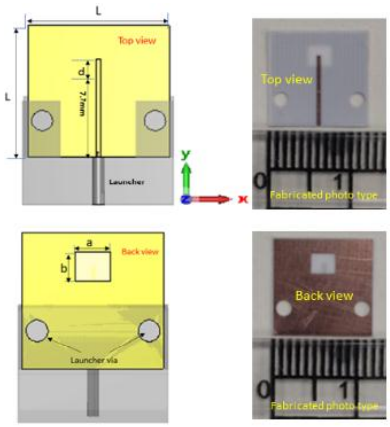

Figure 1: 2D design and an image of the fabricated slot antenna.

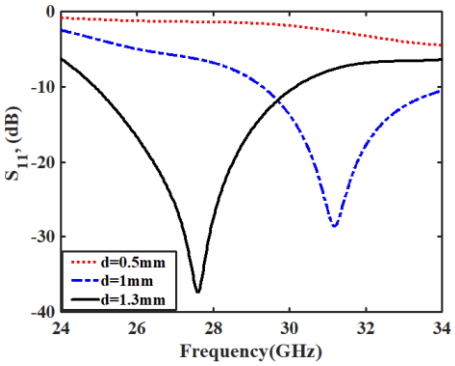

Figure 2: S11 with different values of (d).

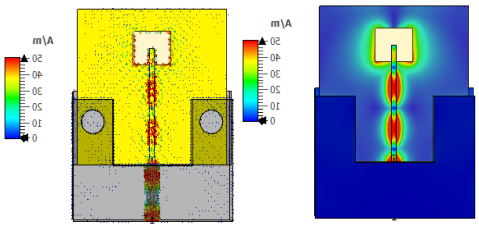

Figure 3: The slot antenna's current distribution.

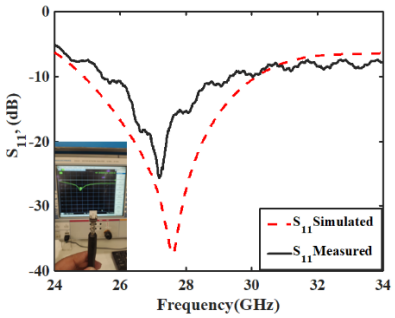

Figure 4: S11 Outcomes of the slot antenna.

The antenna matching changes significantly, as the microstrip length (d) moves between the two values 0.5 and 1.3 mm. At d = 0.5 mm, we lose the antenna matching within the frequency of interest, as displayed in Fig.2. While at d = 1 mm, the frequency band from 29.7 GHz - 34 GHz is obtained with a good level of antenna matching around -28 dB. Finally, at d = 1.3 mm, a frequency band of 26.5 GHz - 30 GHz is produced, with a matching level of less than -37 dB. Figure 3 presents a simulation of the current distribution at 28 GHz. It is seen that the current is collected around the back slot guaranteeing that the radiation of the antenna at the 28GHz frequency band.

The VNA Rohde & Schwarz ZVA 67 is utilized to test the slot antenna through the end launcher, which produces the tested reflection coefficient data displayed in Figure 4. Figure 4 also shows the antenna's calculated frequency spectrum from 25.5 GHz - 30 GHz (4.5 GHz bandwidth), using S11 $\leq$ -10 dB. The tested results suggest a frequency band of 26 GHz - 29 GHz (3 GHz bandwidth) with S11 $\leq$ -10 dB. The simulated and measured results were consistent, as indicated in Figure 4. The measurement setup uses an anechoic chamber, with a slot antenna installed at the receiving end, maintaining a 65 cm distance to meet far-field criteria. A horn antenna, operating at frequencies from 26 to 40 GHz, is installed at the transmitting end. The test antenna is turned around in both two planes and maintains a line-of-sight connection between the two antennas as illustrated in Fig.5. Figure 6 depicts the antenna's realized gain. Within the frequency band, the simulation yields approximately 5 dBi, while the measured results show around 4.7 dBi. Figure 7 shows the radiation patterns of the antenna at 28 GHz. The antenna produces patterns with bidirectional behavior in the two planes, with a strong correlation between the two sets of results.

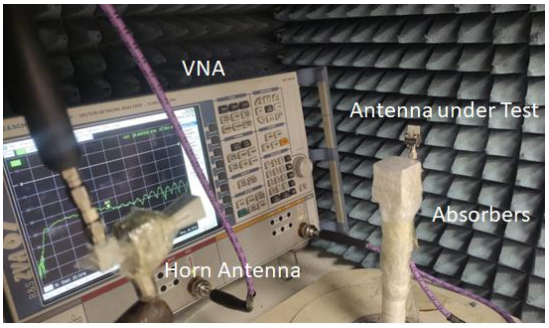

Figure 5: The radiation patterns and gain measuring setup

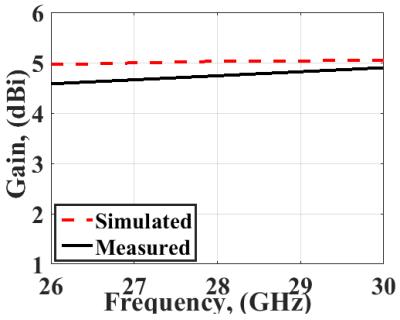

Figure 6: The slot antenna gain

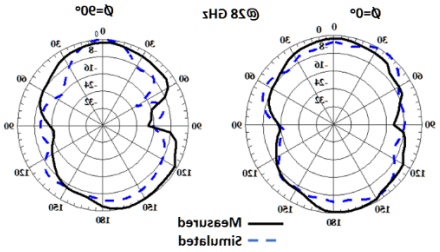

Figure7: The radiation pattern of the antenna

3. 1x2 Antenna Array

To enhance the gain performance compared to the previous antenna, a simple equal-phase feeding network is used to build

1 x 4 linear arrays. This Part covers a 1x 2 sub-arrays; a complete 1 x 4 antenna array is provided in the following part. A simple T-power divider is utilized to feed the array As a Wilkinson energy divider, this type of structure does not need an isolation resistor. Connecting two 50Ω lines in parallel creates approximately 25Ω impedance. A λ/4 transformer with 35.35Ω impedance is connected to the 50Ω feed line. Figure 8 depicts the two views of the 1x2 antenna array in the 2D layout. The design parameters are lf=7, L1=1.9, L2=3, X1=0.4, X2=0.8, X3=4.8, and w=2.2 (all in millimeters). Figure 9 depicts the 1x2 antenna array reflection coefficient. The antenna is simulated with a frequency range varying from 25.6 GHz - 29.8 GHz with S11 ≤ -10 dB, while the tested results accomplished a frequency range from 25.8 GHz - 29.5 GHz. Both simulated and real results are quite consistent. The 1 × 2 array has a gain of 7.4 dBi at 28 GHz.

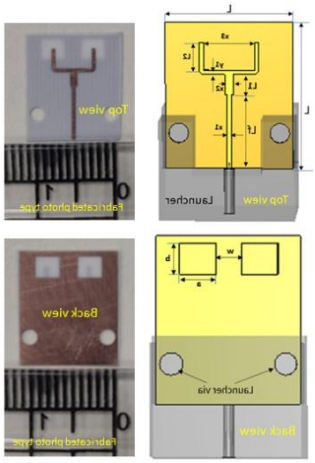

Figure 8: 2D design and an image of the fabricated 1x2 antenna array.

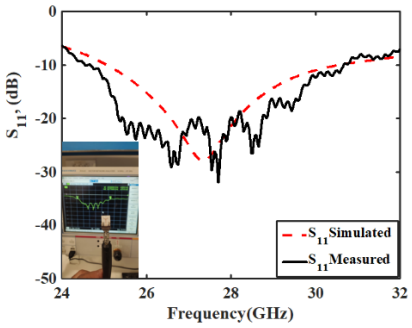

Figure 9: S11 outcomes of the 1x2 antenna array

4. 1x4 Antenna Array

When combining three units of the preceding T-power divider into a 1x2 array, a 1x4 antenna array was formed resulting in good matching and suitable gain characteristics. Optimization parameters for T-dividers are carried out to obtain good results. Figure 10 shows the geometry of the 2D arrangement and a produced photo of the 1x4 antenna array. The design parameters are: L3=1.5, L4=3, Y1=0.4, Y2=0.8, Y3=0.4, X1=10, X2=4.8, X3=4.8, C1=0.4, and C2=0.3 (all in millimeters). Figure 11 depicts the reflection coefficients of a 1 x 4 antenna array. during the measurement process, The Rohde & Schwarz ZVA 67 is used. The antenna's simulated frequency spectrum ranging 26.3 GHz - to 30 GHz. The tested results obtained S11 ≤ -10 dB from 26.6 GHz - 29.8 GHz. Figure 11 shows that the simulated and measured results have good accuracy, which can be attributed to the fabrication procedure. The measurement setup utilizes an anechoic chamber the gain fluctuation versus frequency for the 1 x 4 array is shown in Figure 12. Figure 13 depicts the 2D normal radiation pattern at 28 GHz. The 1 x 4 array creates a bidirectional pattern in two planes that has a narrow beamwidth, demonstrating

good directivity of the array pieces. The two results indicate a positive trend. The simulated peak gain of the array is consistent with the measured measurements. The simulated gain at 28 GHz is 10.8dBi, while the real gain is 10.4dBi.

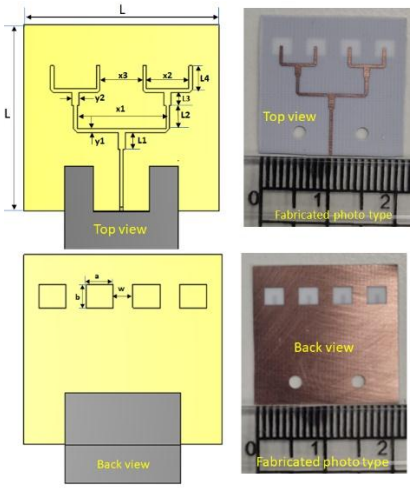

Figure 10: 2D design and an image of the fabricated 1x4 antenna array.

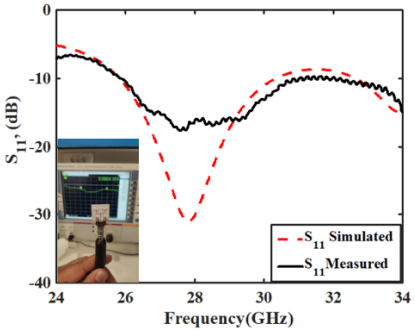

Figure 11: S_{11} Outcomes from Simulations and Measurements of the 1x4 Antenna Array.

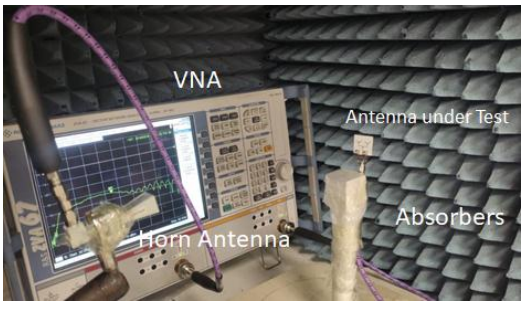

Figure 12: The radiation patterns and gain measuring setup of 1x4 antenna array.

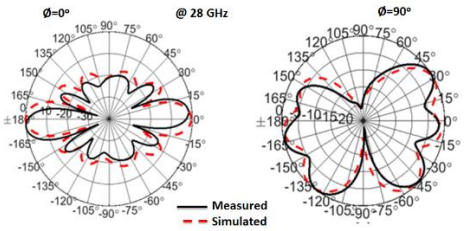

Figure 13: The radiation patterns of the 1x4 antenna.

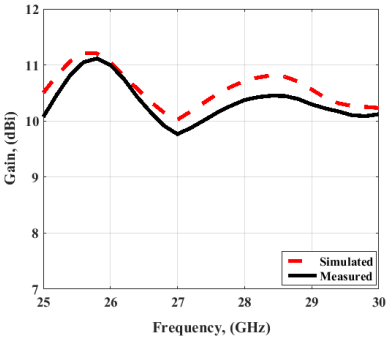

Figure14: the 1x4 antenna array gain

5. Conclusions

A design of slot antenna for upcoming 5G networks with enhanced gain has been proposed. The desired gain enhancement was achieved using a 1x4 array. The proposed antenna measures a total of 12x12 mm. The antenna without a 1x2 or 1x4 array achieved a bandwidth of S11 = -10 dB from 26.5 GHz - 30 GHz and a gain of 5 dBi. When using the 1x2 and 1x4 arrays, the bandwidths achieved with S11 = -10 dB were from 25.6 GHz - 29.8 GHz and from 26.4 GHz - 29.9 GHz, with realized gains of 7.4 dBi and 10.4 dB at 28 GHz, respectively. A good connection between measured and simulated data indicates that the suggested antenna is suitable for impending 5G networks.

References

[1] Ikram, M., et al., *A road towards 6G communication—A review of 5G antennas, arrays, and wearable devices.* 2022. **11**(1): p. 169.
[2] Jabbar, A., et al., *Millimeter-wave smart antenna solutions for URLLC in industry 4.0 and beyond.* 2022. **22**(7): p. 2688.
[3] García Sánchez, M.J.E., *Millimeter-wave communications*. 2020, MDPI. p. 251.
[4] Muñoz, P., et al., *Backhaul-aware dimensioning and planning of millimeter-wave small cell networks.* 2020. **9**(9): p. 1429.
[5] Kiani, S.H., et al., *Eight element side edged framed MIMO antenna array for future 5G smart phones.* 2020. **11**(11): p. 956.
[6] Sabek, A.R., et al., *Minimally coupled two-element MIMO antenna with dual band (28/38 GHz) for 5G wireless communications.* 2022. **43**(3): p. 335-348.
[7] Abdullah, M., S.H. Kiani, and A.J.I.A. Iqbal, *Eight element multiple-input multiple-output (MIMO) antenna for 5G mobile applications.* 2019. **7**: p. 134488-134495.

[8] Abdelaziz, A., H.A. Mohamed, and E.K.J.I.A. Hamad, *Applying characteristic mode analysis to systematically design of 5G logarithmic spiral MIMO patch antenna.* 2021. **9**: p. 156566-156580.
[9] Kim, G. and S.J.I.A. Kim, *Design and analysis of dual polarized broadband microstrip patch antenna for 5G mmWave antenna module on FR4 substrate*. 2021. **9**: p. 64306-64316.
[10] Przesmycki, R., M. Bugaj, and L.J.E. Nowosielski, *Broadband microstrip antenna for 5G wireless systems operating at 28 GHz.* 2020. **10**(1): p. 1.
[11] Zhu, Q., et al., *Substrate-integrated-waveguide-fed array antenna covering 57–71 GHz band for 5G applications.* 2017. **65**(12): p. 6298-6306.
[12] Fatah, S.Y.A., et al., *Design and implementation of UWB slot-loaded printed antenna for microwave and millimeter wave applications.* 2021. **9**: p. 29555-29564.
[13] Nasir, J.A., et al., *A compact low cost high isolation substrate integrated waveguide fed slot antenna array at 28 GHz employing beamforming and beam scanning for 5G applications.* 2018.
[14] Kamal, M.M., et al., *A novel hook-shaped antenna operating at 28 GHz for future 5G mmwave applications.* 2021. **10**(6): p. 673.
[15] Hussain, N., et al., *Compact wideband patch antenna and its MIMO configuration for 28 GHz applications.* 2021. **132**: p. 153612.
[16] Zahra, H., et al., *A 28 GHz broadband helical inspired end-fire antenna and its MIMO configuration for 5G pattern diversity applications.* 2021. **10**(4): p. 405.
[17] Ibrahim, A.A., W.A.J.A.-I.J.o.E. Ali, and Communications, *High gain, wideband and low mutual coupling AMC-based millimeter wave MIMO antenna for 5G NR networks.* 2021. **142**: p. 153990.
[18] Althuwayb, A.A.J.I.J.o.A. and Propagation, *MTM- and SIW-inspired bowtie antenna loaded with AMC for 5G mm-wave applications.* 2021. **2021**(1): p. 6658819.
[19] Ta, S.X., et al., *Broadband printed-dipole antenna and its arrays for 5G applications.* 2017. **16**: p. 2183-2186.
[20] Haraz, O.M., et al., *Dense dielectric patch array antenna with improved radiation characteristics using EBG ground structure and dielectric superstrate for future 5G cellular networks.* 2014. **2**: p. 909-913.
[21] Asaadi, M., I. Afifi, and A.-R.J.I.A. Sebak, *High gain and wideband high dense dielectric patch antenna using FSS superstrate for millimeter-wave applications.* 2018. **6**: p. 38243-38250.
[22] Chatterjee, A., S.K.J.I.T.o.A. Parui, and Propagation, *Frequency-dependent directive radiation of monopole-dielectric resonator antenna using a conformal frequency selective surface.* 2017. **65**(5): p. 2233-2239.
[23] Al-Gburi, A.J.A., et al., *Compact size and high gain of CPW-fed UWB strawberry artistic shaped printed monopole antennas using FSS single layer reflector*. 2020. **8**: p. 92697-92707.
[24] Hocini, A., N. Melouki, and T. Denidni. *Modeling and simulation of an antenna with optimized AMC reflecting layer for gain and front-to-back ratio enhancement for 5G applications*. in *Journal of Physics: Conference Series*. 2020. IOP Publishing.
[25] Wan, W., et al. *Wideband low-profile AMC-based patch antenna for 5G antenna-in-package application*. in *2020 IEEE 70th Electronic Components and Technology Conference (ECTC)*. 2020. IEEE.

Abbreviation and symbols

MMW	**millimeter-wave**
AMC	**artificial magnetic conductor**
FSS	**frequency selective surfaces**